'ROCEEDINGS, Twenty-Second Workshop on Geothermal Reservoir Engineering
Stanford University, Stanford, California, January 27–29, 1997
SGP-TR-155

EFFICIENT NUMERICAL SIMULATION OF NONEQUILIBRIUM MASS AND HEAT TRANSFER IN FRACTURED GEOTHERMAL RESERVOIRS

John W. Pritchett

Maxwell Technologies (formerly S-Cubed)
P.O. Box 23558
San Diego, California, 92123-2355, USA
john@maxwell.com

ABSTRACT

Transient heat and/or fluid mass exchange between the permeable fracture system and the surrounding relatively impermeable country rock can be treated in geothermal reservoir simulators using the "MINC" technique. This approach typically requires about an order of magnitude more computer time than the analogous "porous medium" problem. Under practical conditions, the problem can often be linearized. This paper presents some results using this "linearized MINC" approach. Two situations may be treated — isothermal transient mass transfer between fractures and country rock, and nonequilibrium conductive heat transfer from the country rock to and from the fractures. No assumptions concerning the character of the time-history of fracture pressure or temperature (such as monotonicity, for example) are required. Numerical reservoir simulations using the technique require little more computer time than the analogous porous medium problem.

INTRODUCTION

Twelve years ago, Pruess and Narasimhan (1985) introduced the MINC technique for calculating fluid and heat flow in fractured geothermal reservoirs. Using MINC, macroscopic mass and heat transfer (that is, interchange from one grid block to the next) takes place through the "fracture system", which contains only a relatively small fraction of the reservoir volume but which has most of the permeability. Between these relatively permeable channels is the relatively impermeable country rock, or "matrix region". Mass and heat are exchanged locally between the "fracture zone" and the "matrix region" at the interface between them, and from point to point within the "matrix region" itself in a time-dependent fashion. Each macroscopic grid block is assigned a "representative" element of country rock; within this "matrix region", the subgrid flow is treated as one-dimensional and unsteady, with the representative "matrix region" further discretized spatially into concentric "shells". The governing equations to be solved (conservation of mass and energy) within the "matrix region" are the same as those for the "fracture zone" (except for the limitation to one-dimensional behavior), so that a problem which is mathematically one-dimensional in space becomes essentially two-dimensional (with the spatial degrees of freedom being the x spatial coordinate and "distance into the representative matrix region"); a three-dimensional reservoir problem (x,y,z) becomes four-dimensional. Consequently, the computer time required to solve a practical reservoir problem using the MINC technique is typically at least an order of magnitude greater than that required for the analogous "porous medium" problem. As a result, the practical application of the MINC technique is usually limited to fairly simple problem geometries.

Since the MINC scheme was first introduced, various authors have proposed techniques for obtaining practical results for fractured reservoirs at lower computing costs, basically by linearizing the problem and replacing the discretized subgrid representation with approximate analytic solutions for the time-dependent phenomena talung place within the representative "matrix region" within each macroscopic grid block. Pruess and Wu **(1988)** developed such a technique for the "heat conduction" problem, in which the country rock is taken to be completely impermeable, but non-equilibrium conductive

ieat transfer takes place within the country rock. More 'ecently, Shook (1996) proposed another semi-inalytical technique for treating the "pressure-transient")roblem, in which mass transfer within the country rock s restricted to single-phase isothermal flow with rela-ively small perturbations. Both techniques use semi-inalytical representations for subgrid phenomena, and)wing to the linearity of the description of subgrid flow 'equire little more computer time than the analogous)orous medium problem. This general approach has lrawbacks associated with the assumptions which must)e made for the application of the semi-analytical solu-ions, such as restrictions to monotonic behavior of the ime-variation in conditions in the adjacent fracture zone ınd the like.

The present paper outlines a somewhat different ap-)roach to the problem. The discretized representation)f the original MINC technique is retained, so that con-litions within the subgrid "matrix region" are repre-;ented by concentric "shells", but the equations to be iolved are linearized so that the computational burden)f solving the subgrid problem is minimized. Since the)resent technique is a discretized scheme, it is subject :o the same concerns about resolution and truncation errors that must be kept in mind for any discretized so-lution technique. On the other hand, no restrictions as to fracture-zone time-histories and the like are required.

MATHEMATICAL DEVELOPMENT

For simplicity, the "representative matrix region" to be embedded within the macroscopic grid block is ideal-ized as a sphere, subdivided into concentric shells in such a way that each shell has the same volume (Fig-ure 1). Neither this choice of shell spacing nor the se-lection of spherical geometry is essential to the method—the only requirement is that a one-dimensional representation of some sort be used. The diameter of the representative matrix region (that is, the "fracture spacing") is denoted by λ and the various shells are designated by the subscript i, with the central shell de-noted by $i = 1$ and the outermost shell (adjacent to the fracture zone) by $i = N$.

First, consider the "heat conduction" problem addressed by Pruess and Wu (1988). Transient heat conduction within the matrix region may be represented simply by:

$$\frac{\partial T}{\partial t} = \frac{K}{\rho c_v r^2}\frac{\partial}{\partial r}\left(r^2\frac{\partial T}{\partial r}\right) \qquad (1)$$

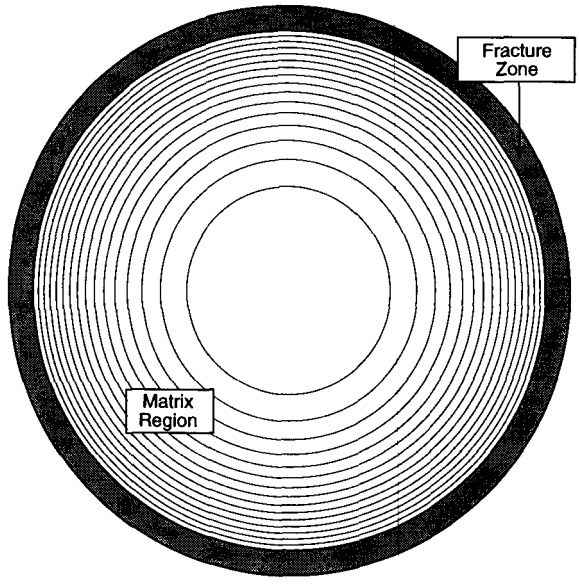

Figure 1. Representation of the matrix region as an assembly of concentric spherical shells, each of equal volume (N = 16).

where T is temperature—a function of radius (r) and time (t)—and K, ρ and c_v are the thermal conductivity, mass density, and heat capacity of the matrix region, respectively. It is useful to rewrite Equation 1 as:

$$\frac{\partial T}{\partial t} = \frac{1}{\tau_e \eta^2}\frac{\partial}{\partial \eta}\left(\eta^2\frac{\partial T}{\partial \eta}\right) \qquad (2)$$

where the time-constant τ_e is defined as:

$$\tau_e = \frac{\rho c_v \lambda^2}{4K} \qquad (3)$$

and the dimensionless radius variable η is given by:

$$\eta = \frac{2r}{\lambda}; \qquad 0 \le \eta \le 1 \qquad (4)$$

Note that the heat flow from the fracture zone into the matrix region (per unit volume of matrix region) is given by:

$$\dot{e} = \frac{3\rho c_v}{\tau_e}\left[\frac{\partial T}{\partial \eta}\right]_{\eta=1} \qquad (5)$$

Next, consider the "pressure-transient" problem examined by Shook **(1996).** In this case, the essential governing equation may be written:

$$\frac{\partial P}{\partial t} = \frac{k}{\phi C \mu r^2} \frac{\partial}{\partial r}\left(r^2 \frac{\partial P}{\partial r} \right) \tag{6}$$

where P is the fluid pressure (a function of r and t), k represents the absolute permeability of the matrix region, ϕ is matrix region porosity, C is the total system compressibility (rock plus fluid), and μ is fluid viscosity. This expression may also be written as:

$$\frac{\partial P}{\partial t} = \frac{1}{\tau_m \eta^2} \frac{\partial}{\partial \eta}\left(\eta^2 \frac{\partial P}{\partial \eta} \right) \tag{7}$$

The time-constant for mass flow is just:

$$\tau_m = \frac{\phi C \mu \lambda^2}{4k} \tag{8}$$

and the spatial variable η is given by Equation **4** (above). The mass flow rate per unit matrix region volume from the fracture zone into the matrix region is given by:

$$\dot{m} = \frac{3\phi \rho_f C}{\tau_m}\left[\frac{\partial P}{\partial \eta} \right]_{\eta=1} \tag{9}$$

where ρ_f is the mass density of the liquid within the matrix region.

Thus, both the "heat conduction" and the "pressure transient" cases are of the same general form, with the redistribution of the pertinent field variable **Q** (pressure or temperature) within the matrix region governed by:

$$\frac{\partial Q}{\partial t} = \frac{1}{\tau \eta^2} \frac{\partial}{\partial \eta}\left(\eta^2 \frac{\partial Q}{\partial \eta} \right) \tag{10}$$

and with the interchange of mass or energy between the matrix region and the fracture zone dictated at each instant of time by a source/sink term of the form:

$$\dot{q} = \frac{3 \times \text{constant}}{\tau}\left[\frac{\partial Q}{\partial \eta} \right]_{\eta=1} \tag{11}$$

The essential problem is therefore to devise a procedure for solving Eq. **10** on the region $0 \le \eta \le 1$ subject to arbitrary initial conditions and to **a** time-dependent boundary value dictated by conditions within the fracture zone at $\eta = 1$. The solution will be accomplished (as for the macroscopic reservoir problem) using a series of finite time-steps and a fully implicit approach — the time-step size for the "subgrid" problem is taken to be the same as for the "macroscopic" problem. Let Q^n represent the distribution of **Q** at $t = t^n$, and let Q^{n+1} represent the Q-distribution a short time later, at $t = t^{n+1} = t^n + \Delta t$. The objective is to solve for the Q^{n+1} distribution using the following time-discretized form of Eq. **10:**

$$Q^{n+1} = Q^n + \left(\frac{\Delta t}{\tau} \right) \frac{1}{\eta^2} \frac{\partial}{\partial \eta}\left(\eta^2 \frac{\partial Q^{n+1}}{\partial \eta} \right) \tag{12}$$

Spatial discretization follows usual practice. Q_i denotes the value of **Q** in shell number i; the space-discretized form of Equation **12** is:

$$Q_i^{n+1}\left(1 + L_i + R_i\right) - Q_{i-1}^{n+1} L_i - Q_{i+1}^{n+1} R_i = Q_i^n \tag{13}$$

where

$$L_i = \left(\frac{\Delta t}{\tau} \right)\left(\frac{\eta_{i-1/2}}{\eta_i} \right)^2 \Big/ \left(\Delta \eta_i \Delta \eta_{i-1/2} \right) \tag{14}$$

$$R_i = \left(\frac{\Delta t}{\tau} \right)\left(\frac{\eta_{i+1/2}}{\eta_i} \right)^2 \Big/ \left(\Delta \eta_i \Delta \eta_{i+1/2} \right) \tag{15}$$

where Q_i is considered to be "located" at the midpoint of shell i, and where

$$\eta_{i+1/2} = \text{outer dimensionless radius of shell } i \quad (\eta_{1/2} = 0; \quad \eta_{N+1/2} = 1) \tag{16}$$

$$\eta_i = \frac{1}{2}\left(\eta_{i+1/2} + \eta_{i-1/2} \right) \tag{17}$$

$$\Delta \eta_i = \eta_{i+1/2} - \eta_{i-1/2} \tag{18}$$

$$\Delta\eta_{i+1/2} = \eta_{i+1} - \eta_i \qquad (19)$$

The boundary condition ($Q = Q_B(t)$ at $\eta = 1$) is imposed by setting $\Delta\eta_{N+1/2} = \Delta\eta_N$ and $Q_{N+1}^{n+1} = 2Q_B^{n+1} - Q_N^{n+1}$. Therefore, for $i = N$, Equation 13 becomes:

$$Q_N^{n+1}(1 + L_N + 2R_N) - Q_{N-1}^{n+1}L_N = Q_N^n + 2R_N Q_B^{n+1} \qquad (20)$$

It may easily be shown that the solution of the above system of equations (Equation 13 for $1 \le i \le N-1$; Equation 20 for $i = N$) for the Q_i^{n+1} may be written as a simple polynomial as follows:

$$Q_i^{n+1} = B_i Q_B^{n+1} + \sum_{j=1}^{N} A_{ij} Q_j^n \qquad (21)$$

where Q_B^{n+1} is the imposed boundary value of Q (associated with conditions prevailing within the fracture zone) and where the coefficients (B_i, A_{ij}) may be obtained by solving N + 1 auxiliary problems of the general form of Equations 13 and 20. The first auxiliary problem (lower right frame in Figure 2) involves solving for the new value of Q in each shell subject to initial conditions $Q^n = 0$ everywhere and boundary condition $Q_B = 1$ and setting this value equal to the B coefficient; that is,

$$B_i(1 + L_i + R_i) - B_{i-1}L_i - B_{i+1}R_i = 0 \quad (\text{for } 1 \le i \le N-1) \qquad (22a)$$

$$B_N(1 + L_N + 2R_N) - B_{N-1}L_N = 2R_N \qquad (22b)$$

Solving Eq. 22 for the B, amounts to solving a tridiagonal matrix. The remaining N auxiliary problems provide the A_{ij} coefficients. Successively setting $j = 1, 2, 3, \ldots, N$, the following problem is solved for the A_{ij}:

$$A_{ij}(1 + L_i + R_i) - A_{i-1\,j}L_i - A_{i+1\,j}R_i = \delta_{ij} \quad (\text{for } 1 \le i \le N-1) \qquad (23a)$$

$$A_{Nj}(1 + L_N + 2R_N) - A_{N-1\,j}L_N = \delta_{Nj} \qquad (23b)$$

where δ_{ij} equals 1 if $i = j$ and equals zero otherwise. That is, the A_{ij} are the new values of Q_i which result from imposing initial conditions $Q_i^n = 1$ for $i = j$ and $Q_i^n = 0$ for $i \neq j$, and boundary condition $Q_B = 0$ (see remaining frames of Fig. 2).

It is of particular importance to note that, for a particular value of N and a specified shell-spacing pattern, the coefficients B_i and A_{ij} will depend only upon the ratio $\Delta t / \tau$; in the example illustrated in Figure 2, N = 8 (a fairly small value selected for clarity of presentation) and $\Delta t = 0.04\,\tau$. Therefore, the total number of coefficient sets (A_{ij}, B_i) which must be computed and stored during the course of a calculation need not exceed the total number of different values of the $\Delta t / \tau$ ratio which will be encountered. Usually, the number of different values of τ involved will be vastly smaller than the number of macroscopic grid blocks—usually, two or three different values will suffice, and often only one is needed. Now, if the time-step size is constant (or takes on at most only a few discrete values), then the total number of recalculations of coefficient sets (solutions of Equations 22 and 23) required will be vastly less than the product of the number of grid blocks and the number of time-steps. Accordingly, the computational burden associated with calculating the A_{ij} and B_i coefficients will be negligible.

To summarize, the procedure at each computational time-step is as follows:

Step 1: Check and see if the time-step size has changed (or if this is the first time-step). If so, recalculate the A_{ij} and B_i coefficients using Equations 22 and 23. Otherwise, proceed.

Step 2: Compute mass and/or energy "source terms" for application to the solution for conditions in the fracture zone at the next time level using a finite-difference analogue of Equation 11. The source-rate term in the fracture zone will be proportional to the quantity $(Q_N^{n+1} - Q_B^{n+1})$. Using Equation 21, this means that:

$$\text{Source term} \sim -\sum_{j=1}^{N} A_{Nj} Q_j^n - (1 - B_N) Q_B^{n+1} \qquad (24)$$

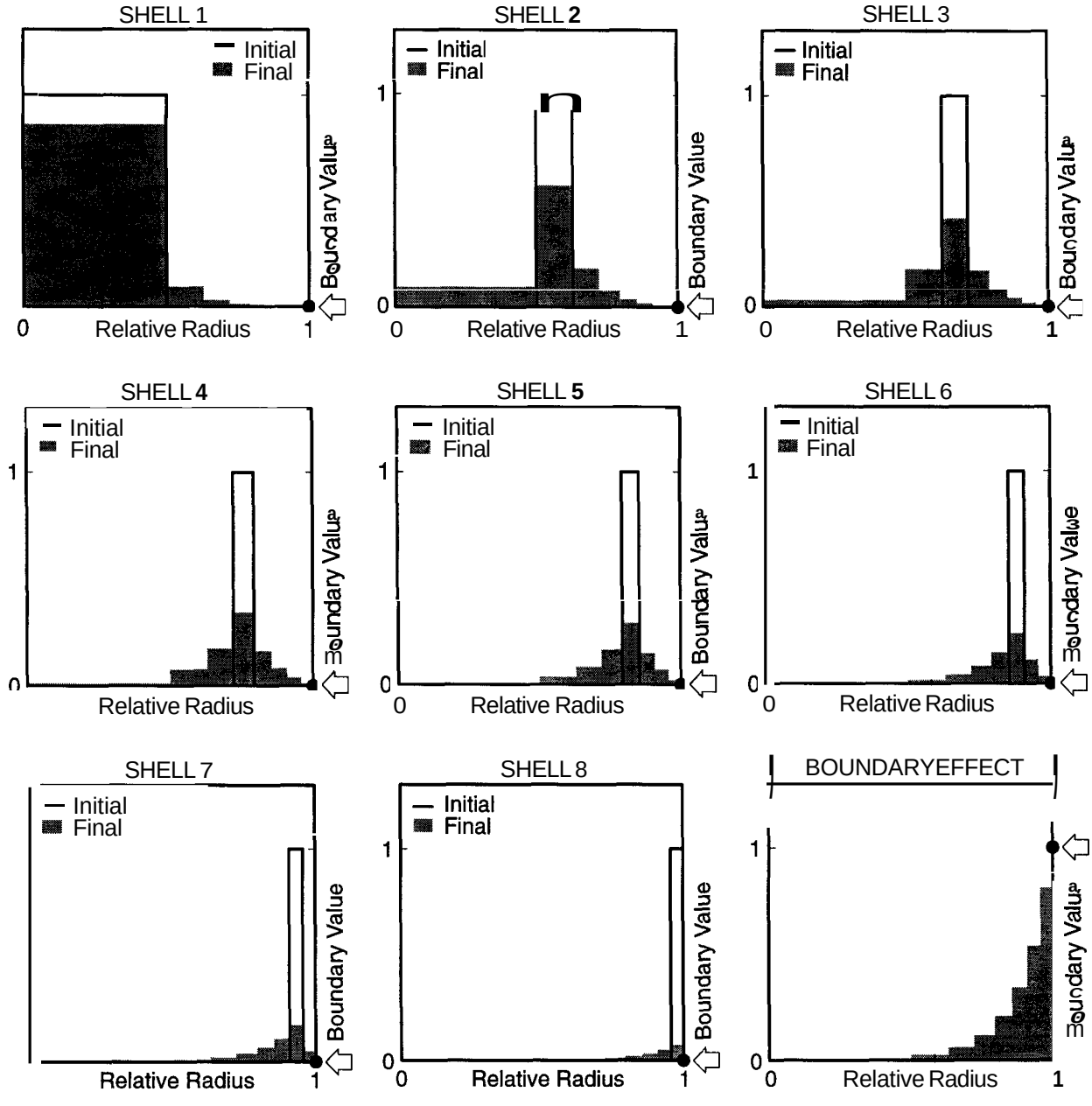

Figure 2. Calculation procedure for coefficients A, and B_i for the particular case N = 8, Δt = 0.04 τ.

All quantities in Equation 24 are known at this stage cept for the "new" value of the boundary value Q; this is the same as the "fracture zone" value of Q (pressure or temperature). Accordingly, the source term to applied to the fracture zone solution in each macropic grid block is a simple linear function of fracture ne pressure or temperature.

Step 3: Compute the new state of the system in the fracture zone using the general-purpose non-linear reservoir simulator as usual, imposing the linear source/sink terms in each grid block calculated in Step 2 above. This yields values for fracture zone pressure and temperature at the new time level for each macroscopic grid block (Q_B^{n+1}).

Step 4: For each macroscopic grid block, calculate and store the new values of Q in each subgrid shell using Equation 21.

Virtually all of the computer time will be consumed by Step 3 (the nonlinear problem). The total amount of computer time required by Steps 2 and 4 together per macroscopic grid block per time step will be given approximately by

$$\text{CPU time} = 2\,(N+1)^2 / \text{Speed}$$

For example, if $N = 8$ (as in Figure 2), if we consider a reservoir model containing 5000 grid blocks and carry it forward for 1000 time-steps using a small desktop scientific workstation capable of 100 megaflop performance, the total CPU time involved for Steps 2 and 4 amounts to only about eight seconds altogether. For such a problem, the calculations involved in Step 3 are likely to take several hours.

APPLICATIONS

Unlike the methods proposed by Pruess and Wu (1988) and by Shook (1996), the present technique retains the spatially-discretized character of the original MINC formulation (Pruess and Narasimhan, 1985). Accordingly, it is important to examine the effects of finite shell spacing upon the accuracy of the method. Consider an assembly of N concentric shells such as that depicted in Figure 1, with the shell spacings arranged so that the volume of each shell is the same. If the method proposed above is applied to the heat conduction problem with uniform temperature T_1 within the sphere at $t = 0$ and boundary temperature maintained at T_2, the calculated results are as depicted in Figure 3 for the volume-averaged temperature within the assembly as a function of time. For these calculations, the computational time-step was deliberately kept very small to isolate the effects of spatial discretization. The "exact" solution to the problem may be obtained from Carslaw and Jaeger (1959). As Figure 3 shows, if $N = 1$ (no subdivisions of the matrix region at all—equivalent to a Warren-Root model), representation of the thermal transient is rather poor. Even if only a few shells are provided, however, results are surprisingly good. For practical purposes, it appears that $N = 8$ (as in Figure 2) should probably be regarded as a lower limit on N. Since large values of N impose little computational penalty, there is no particular reason to restrict the number of shells unduly.

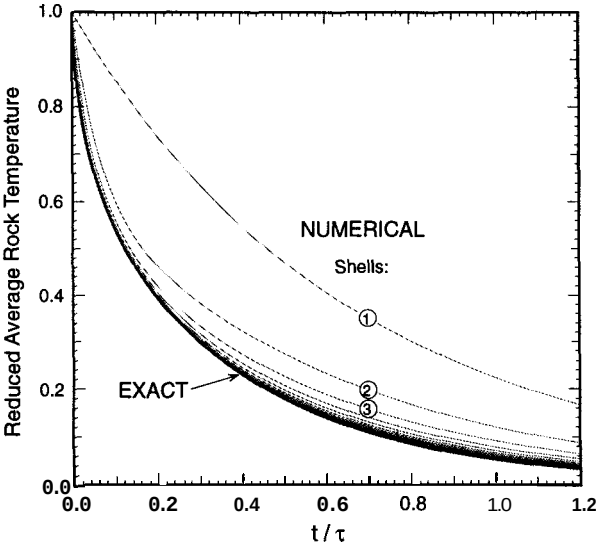

Figure 3. Change in reduced volume-average temperature $\left[(\bar{T} - T_1)/(T_2 - T_1)\right]$ vs. time for initially isothermal sphere subjected to a fixed-temperature outer boundary condition—influence of subgrid resolution on results.

A few computed results for a practical reservoir engineering application of the present method are depicted in Figure 4. A match to a seven-year production history is involved. The field is liquid-dominated and relatively small in size, with about a dozen wells and a flash-steam plant. Shortly after the beginning of field exploitation, discharge enthalpies began declining at an alarming rate. Since the enthalpy decline was accompanied by a substantial rise in produced fluid chloride, the operator correctly reasoned that the reinjection wells were located too close to the production wells, and began a program of relocation of the injection wellfield which took place between years 2 and 4. This strategy was largely successful; discharge enthalpies began to stabilize, and the chloride of the produced brine began to decline, as indicated by the measured data shown in Figure 4.

The modeling process involved the development of a "natural-state" model for the field (a mathematical representation which is essentially steady, with good agreement between measured underground pressures and temperatures and computed values). Once an adequate natural-state model was developed (using a porous-medium model; in steady-state, a MINC model will produce the same results as a porous medium model), the history-match was undertaken. As Figure 4B shows,

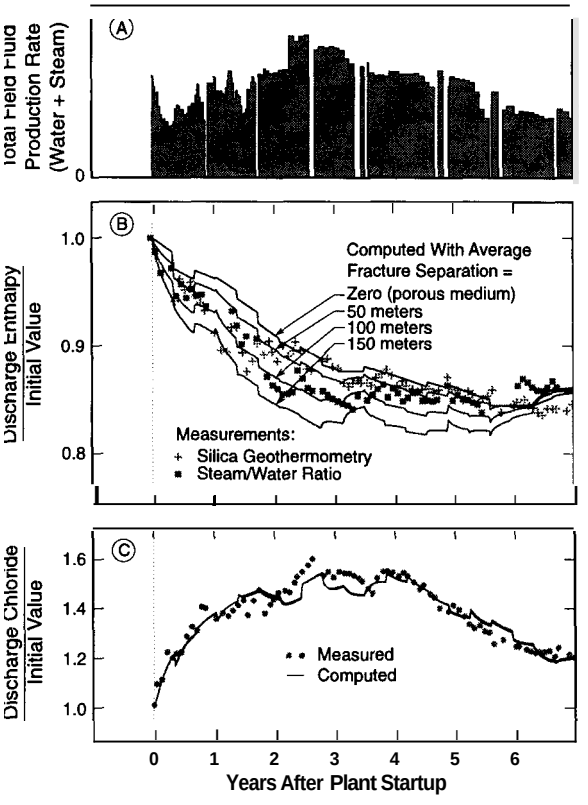

Figure 4. ***Effect of average fracture spacing upon history-match for a small liquid-dominated geothermal field.***

if the porous medium representation was employed for the history-match portion of the study, it was not possible to reproduce the rapid early decline in discharge enthalpy adequately. Accordingly, the "linearized MINC" approach was tried ("heat conduction" model with impermeable country rock). Figures 4B and 4C show results for calculations which differ only in the value of the average fracture separation assumed. Changing the average fracture separation has negligible effects upon the discharge chloride history, but the early part of the discharge enthalpy history is strongly dependent upon average fracture separation; as fracture separation increases, the initial rate of enthalpy decline likewise increases. Based on these results, we concluded that the actual average fracture separation in the field is between 50 and 100 meters, which is consistent with drilling log data.

For simplicity, the above field calculations were each carried out using a single value of the fracture separation (that is, a single value of the time-constant τ_e; see Equation **3)** which was treated **as** uniform throughout the field. The present method lends itself readily to treatment of systems for which the fracture separation is heterogeneous in at least two senses. First, of course, different values of z may be assigned to different groups of grid blocks representing different "rock formations" or other structural features. Thus, for example, part of the reservoir may be treated as a "porous medium", another part may be treated as a "fractured medium" with a large average fracture separation, while yet another might have an intermediate description. Furthermore, the "heat-conduction'' version of the technique might be appropriate in some parts of the computational grid, while the "pressure-transient" version might be useful in others. There is no particular reason, moreover, why both treatments cannot be simultaneously applied within a single grid block.

"Microscale heterogeneity" is another sense in which the technique is well-suited for treating complex systems. In reality, fractured rock masses are usually not regular structures with a uniform spacing between the fractures, but contain **an** entire spectrum of fragment sizes. Using the present technique, it is perfectly possible to assign multiple values of τ to an individual macroscopic grid block, with each different value of τ assigned a particular fraction of the grid block volume. In this way, continuous distributions of fracture spacings can be approximated. Owing to the high computational efficiency of the present method, such calculations involving distributions of fracture spacings within individual grid blocks as well as large-scale heterogeneities in the properties of the fracture system may be carried out at little additional cost beyond that of the analogous porous medium problem.

REFERENCES

Carslaw, H. S. and J. C. Jaeger (1959), "Conduction of Heat in Solids", Oxford Univ. Press, Oxford, England, Second Edition.

Pruess, K. and T. N. Narasimhan (1985), "A Practical Method for Modeling Heat and Fluid Flow in Fractured Porous Media", Soc. Petrol. Eng. J., ***25,*** pp. 14–26.

Pruess, K. and Y. S. Wu (1988), "A Semi-Analytical Method for Heat Sweep Calculations in Fractured Reservoirs", Proc. Thirteenth Workshop on Geothermal Reservoir Engineering, Stanford University, Stanford, California, pp. 219–224.

Shook, G. M. (1996), "Matrix-Fracture Interactions in Dual Porosity Simulation", Geothermal Resources Council Transactions 1996 Annual Meeting, Portland, Oregon, pp. 851–857.